Numerov's method for the one dimensional time-independent Schrödinger equation. Harmonic oscillator, double-well and the Morse potential.

Reinaldo Magallanes Saunders*

October 2020

1 Introduction.

The main objective of this assignment is to approximate solutions to the one dimensional time-independent Schrödinger equation for bound states in a potential. This will be done using a script written in Python that implements Numerov's algorithm.

2 Numerov's Algorithm.

Numerov's method is used to integrate second-order differential equations, with suitable initial conditions, of the general form:

$$\frac{d^2y}{dx^2} = -g(x)y(x) + s(x) \quad , \quad y(x_0) = y_0 \quad , \quad y'(x_0) = y'_0. \tag{1}$$

It assumes that the equation can be discretized and integrated. That is, it can be written on a suitable finite grid of equispaced points and solved, the solution given over the grid.

The Schrödinger equation

$$-\frac{\hbar^2}{2m}\frac{d^2}{dx^2}\Psi(x) = [E - V(x)]\Psi(x) \tag{2}$$

has this form, with

$$g(x) = \frac{2m}{\hbar^2}[E - V(x)] \quad and \quad s(x) = 0 \tag{3}$$

If x_i are the points on the grid and $y_i = y(x_i)$ the values of the function at those points, Numerov's formula, for $s(x) = 0$, is given by[1]:

*e-mail: rei.magallanes@gmail.com

$$y_{n+1}\left[1+g_{n+1}\frac{(\Delta x)^2}{12}\right]=2y_n\left[1-5g_n\frac{(\Delta x)^2}{12}\right]-y_{n-1}\left[1+g_{n-1}\frac{(\Delta x)^2}{12}\right]+O[(\Delta x)^6] \quad (4)$$

where $\Delta x = x_{i+1} - x_i$ and $g_i = g(x_i)$. This gives y_{n+1} in terms of y_n and y_{n-1}, meaning that, under iteration, we can obtain the function over the entire grid. We can introduce an auxiliary quantity f_n, defined as

$$f_n = 1 + g_n\frac{(\Delta x)^2}{12} \quad (5)$$

to write Numerov's formula as

$$y_{n+1} = \frac{(12-10f_n)y_n - y_{n-1}f_{n-1}}{f_{n+1}} \quad (6)$$

First thing to notice about solving equation (2) is that we need to find pairs $(E, \Psi(x))$ that satisfy the equation simultaneously. This will be done by setting a trial value for E and searching for the desired value using bisection. By calculating y for this trial energy, we can check if the number of nodes for this y matches the number of nodes of the solution, since this number is an input. Then, we can change the boundaries for the energy accordingly and repeat this process until we get the desired value. The initial value for E was taken, in every case, to be the average of the potential valued at the boundaries of the interval where equation (2) is to be solved.

Also, since the algorithm needs two initial values, namely y_0 and y_1, we need to set them. This will be done taking into account certain properties of the potentials and expected behaviour of the wave function at those points.

Finally, as we will show later, wave functions obtained with this algorithm are *not* normalizable. So, because of this, we take some liberties when choosing the initial values for the iteration since the only thing that could be said about those wave functions is whether or not the overall shape of the graph is compatible with known solutions.

3 The Harmonic Oscillator.

For a particle of mass m under a one-dimensional harmonic potential $V(x) = \frac{1}{2}m\omega^2x^2$, the time-independent Schrödinger equation can be written as:

$$\frac{d^2}{dx^2}\Psi(x) = -\left(\frac{2mE}{\hbar^2} - \frac{m^2\omega^2x^2}{\hbar^2}\right)\Psi(x) \tag{7}$$

Introducing the following dimensionless variables:

$$\chi = \sqrt{\frac{m\omega}{\hbar}}x \quad and \quad \varepsilon = \frac{E}{m\omega} \tag{8}$$

equation (7) can be written as

$$\frac{d^2}{d\chi^2}\Psi(\chi) = -(2\varepsilon - \chi^2)\Psi(\chi) \tag{9}$$

Exact solutions, normalized in χ, for this equation are known[2], and are given by:

$$\Psi_n(\chi) = \frac{e^{-\frac{\chi^2}{2}}H_n(\chi)}{\sqrt{n!2^n\sqrt{\pi}}} \quad , \quad \varepsilon_n = n + \frac{1}{2} \quad for \quad n = 0, 1, 2, ... \tag{10}$$

where $H_n(\chi)$ is the n-th order Hermite polynomial.
So, in this case, the $g(x)$ function in (1) is given by

$$g(\chi) = 2\varepsilon - \chi^2 \tag{11}$$

This is why, in the code, the 'potential' is treated as $V(\chi) = \chi^2$ and the algorithm converges to twice the value of ε. However, in the graphs that follow, this was taken into account and the value we want of ε is shown.

The algorithm will search for a solution $\Psi_n(\chi)$ with the desired number of nodes, which is given by n. Iteration will be done for $\chi \geq 0$ and, since the potential is even, we will use the fact that solutions have definite parity to construct $\Psi_n(\chi)$ for $\chi < 0$ via

$$\Psi_n(-\chi) = (-1)^n\Psi_n(\chi) \tag{12}$$

This ties directly into the choice of the starting points for the iteration. Known behaviour near zero is used, which depends on the number of nodes.

For an even number of nodes, y_0 is arbitrary while y_1 is given by (6) with $f_{-1} = f_1$ and $y_{-1} = y_1$. We chose:

$$y_0^{even} = \frac{1}{H_n(0)} \quad , \quad y_1^{even} = \frac{(12 - 10f_0)y_0}{2f_1} \tag{13}$$

For an odd number of nodes, y_0 has to be zero, and y_1 is arbitrary. To preserve the overall shape of the graph of the exact solution, we chose:

$$y_0^{odd} = 0 \quad , \quad y_1^{odd} = \frac{1}{H_n(\chi_1)} \tag{14}$$

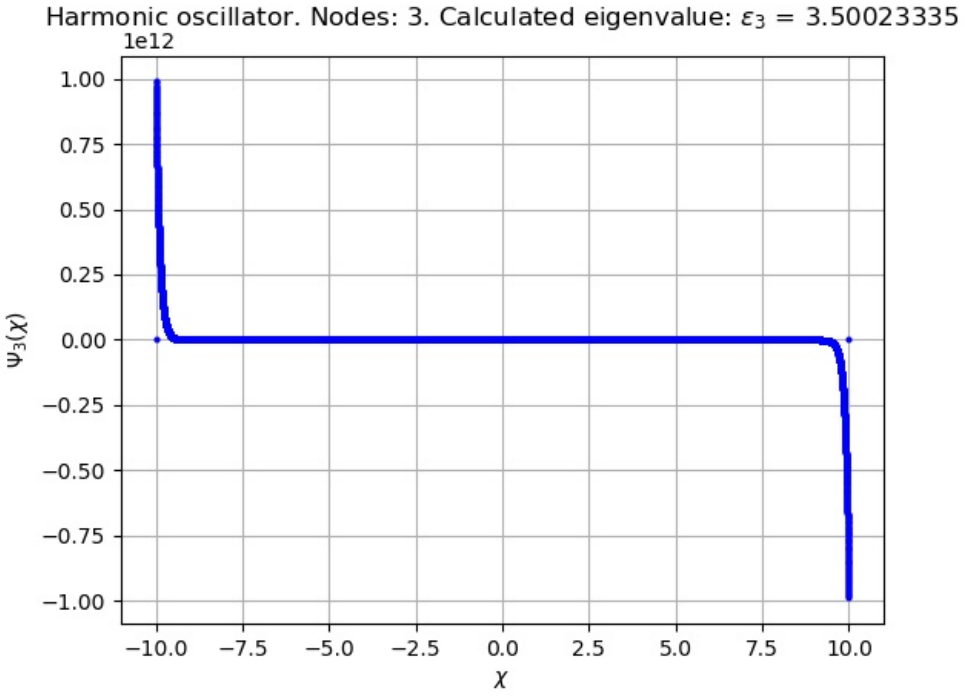

Figure 1: Example to show divergent behaviour of the wave function obtained.

where χ_1 is the second point over the grid.

As mentioned previously, the obtained solutions won't be normalizable. This is because, when the wave function is vanishingly small, the algorithm is not stable. This can be seen in Figure 1.

This behaviour can be seen in solutions for both the harmonic potential and the double-well potential. For this reason, the graphs shown for both of these potentials are restricted to an interval where we can actually see what the solution looks like. As for the Morse potential, this behaviour can be seen, but it's not as severe, so those graphs are not restricted to a specific interval.

For every calculation, the value for the upper bound for χ was chosen to be 10 with 15000 grid points. For the graphs, the interval $[-6, 6]$ was taken. This was chosen because it allows for the solution to be compared with the exact result. This can be seen in Figures 2, 3, 4, 5 and 6.

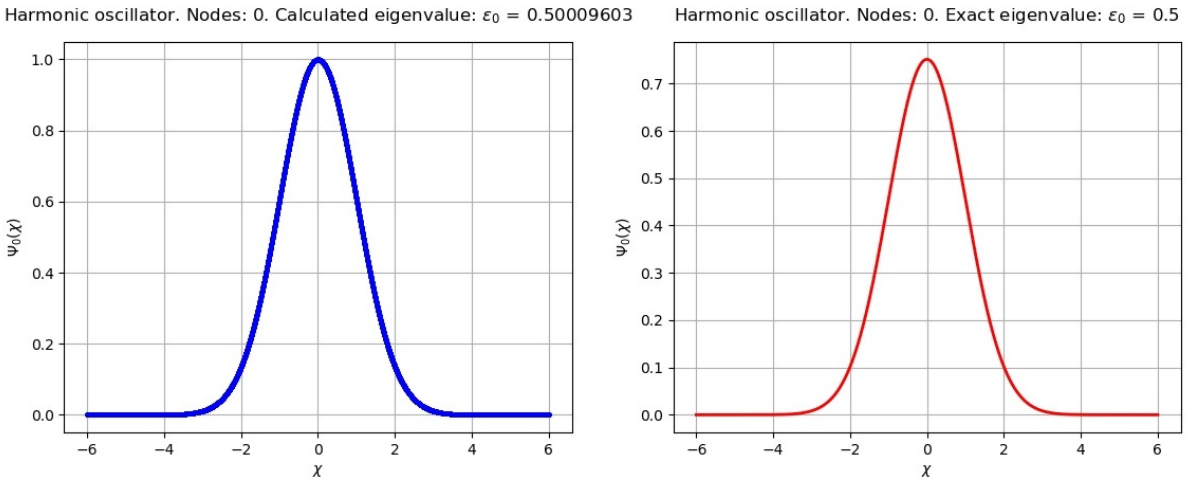

Figure 2: Solution of (9) for $n = 0$. Left: solution obtained. Right: exact solution.

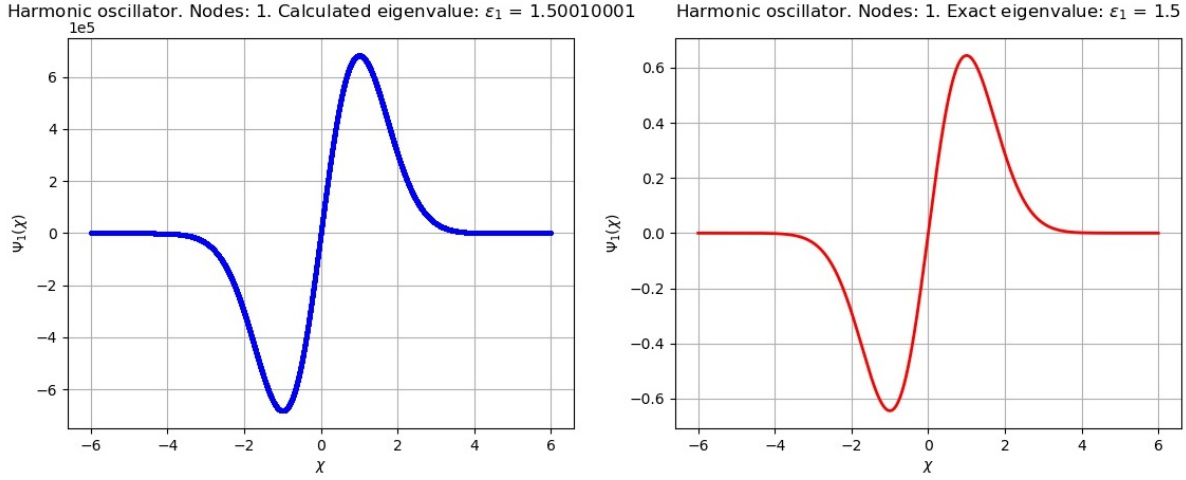

Figure 3: Solution of (9) for $n = 1$. Left: solution obtained. Right: exact solution.

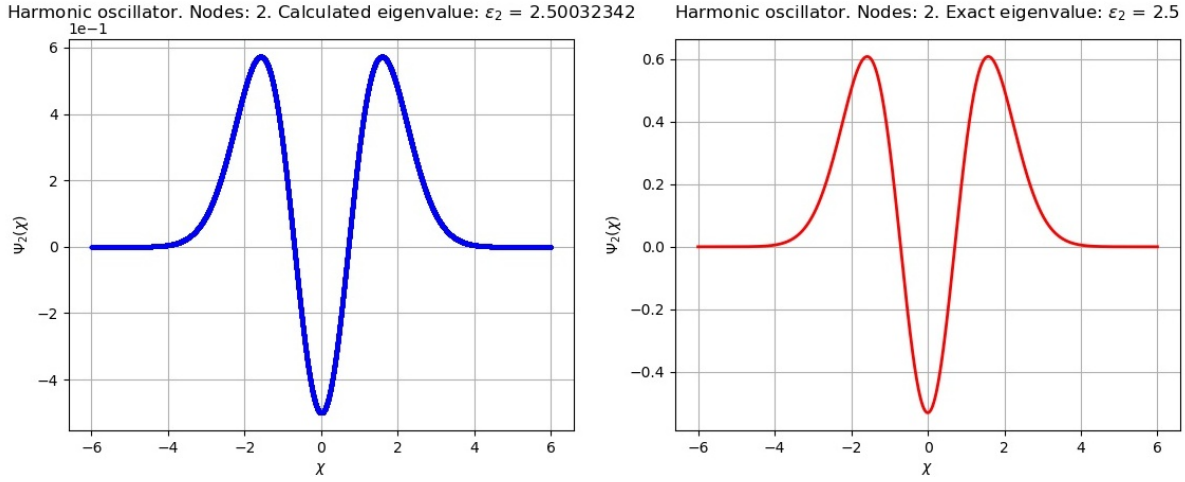

Figure 4: Solution of (9) for $n = 2$. Left: solution obtained. Right: exact solution.

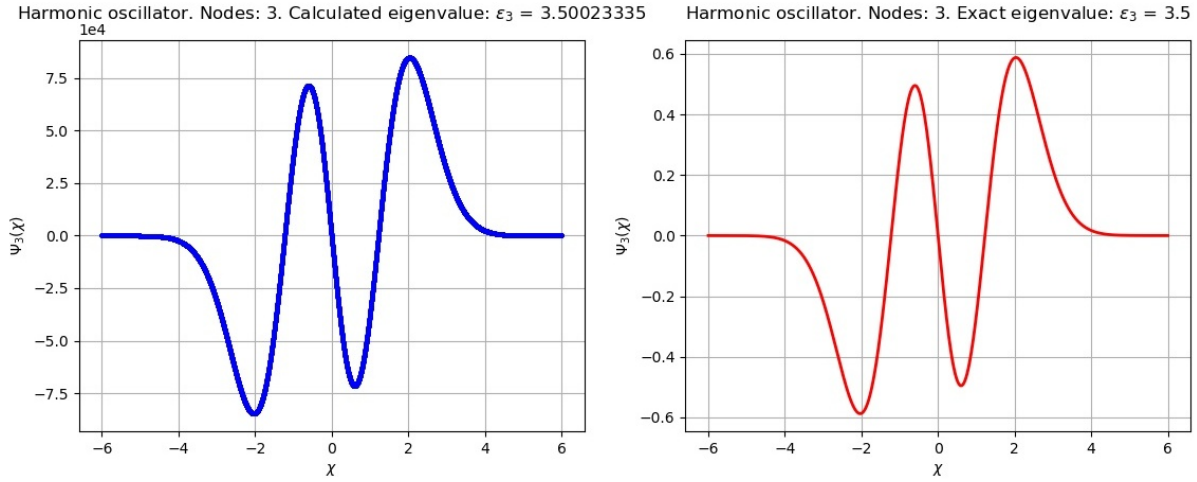

Figure 5: Solution of (9) for $n = 3$. Left: solution obtained. Right: exact solution.

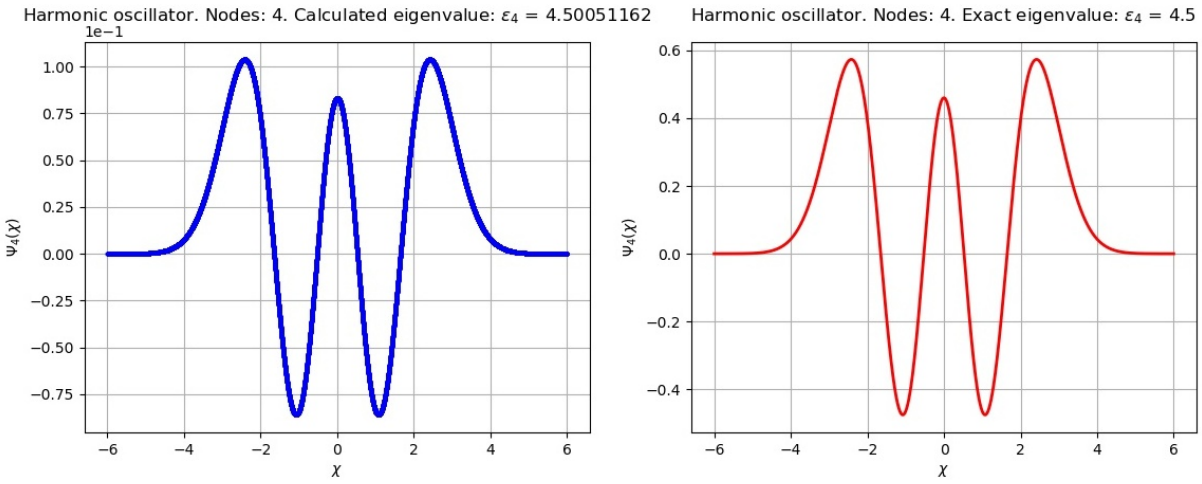

Figure 6: Solution of (9) for $n = 4$. Left: solution obtained. Right: exact solution.

4 Double-well Potential.

For the double-well potential, we take a potential of the form

$$V(x) = \varepsilon \left[\left(\frac{x}{\delta} \right)^4 - 2 \left(\frac{x}{\delta} \right)^2 + 1 \right] \quad , \quad \varepsilon, \delta > 0 \tag{15}$$

We can write the Schrödinger equation for a particle of mass m under the influence of this potential as:

$$\frac{d^2}{dx^2}\Psi(x) = -\left(\frac{2mE}{\hbar^2} - \frac{2m\varepsilon}{\hbar^2} \left[\left(\frac{x}{\delta} \right)^4 - 2 \left(\frac{x}{\delta} \right)^2 + 1 \right] \right) \Psi(x) \tag{16}$$

Using the change of variables

$$\chi = \sqrt{\frac{2m}{\hbar^2}} x = bx \tag{17}$$

we can write

$$\frac{d^2}{d\chi^2}\Psi(\chi) = -\left(E - \varepsilon \left[\left(\frac{\chi}{\frac{\delta}{b}} \right)^4 - 2 \left(\frac{\chi}{\frac{\delta}{b}} \right)^2 + 1 \right] \right) \Psi(\chi) \tag{18}$$

With this expression, we choose

$$\varepsilon = \frac{1}{2} \quad and \quad \frac{\delta}{b} = \sqrt{3} \tag{19}$$

and thus

$$\frac{d^2}{d\chi^2}\Psi_n(\chi) = -\left(E_n - \frac{1}{2} \left[\frac{\chi^4}{9} - 2\frac{\chi^2}{3} + 1 \right] \right) \Psi(\chi) \tag{20}$$

where n is the number of nodes. The potential in (20) can be seen in Figure 7.

We expect solutions to this equation to not be too dissimilar from the solutions to the harmonic potential[3]. So, the initial values for iteration and the construction of solutions for negative values of χ are the same as before.

The parameters taken for iteration were also the same as in the harmonic potential. Results can be seen in Figures 8, 9, 10, 11 and 12.

One thing worth mentioning is that for the ground state, the maximum is not reached at $\chi = 0$[3]. This is barely noticeable in Figure 8.

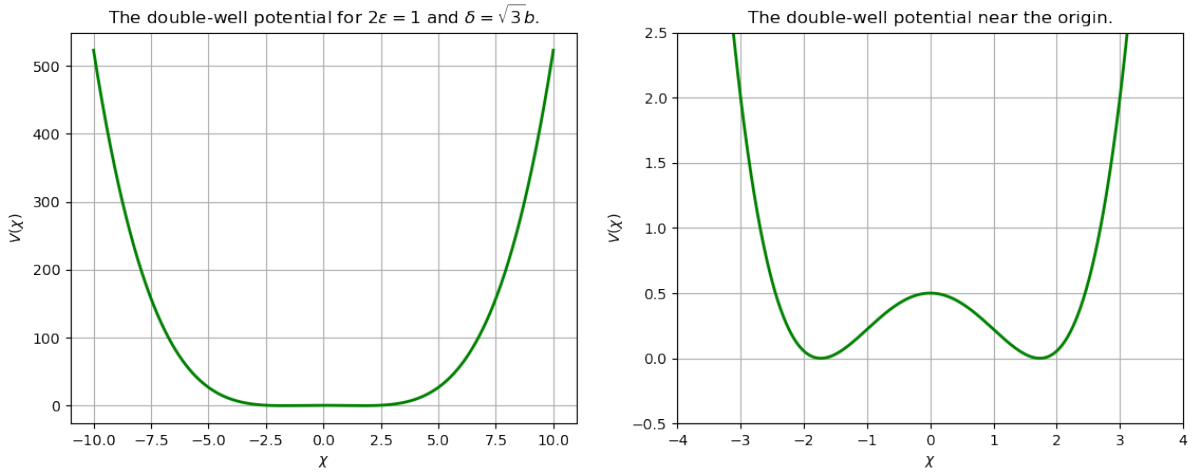

Figure 7: Double-well potential as written in (20).

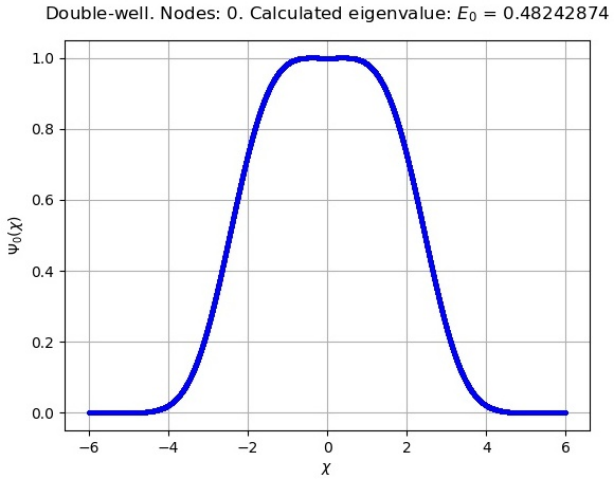

Figure 8: Solution of (20) for $n = 0$.

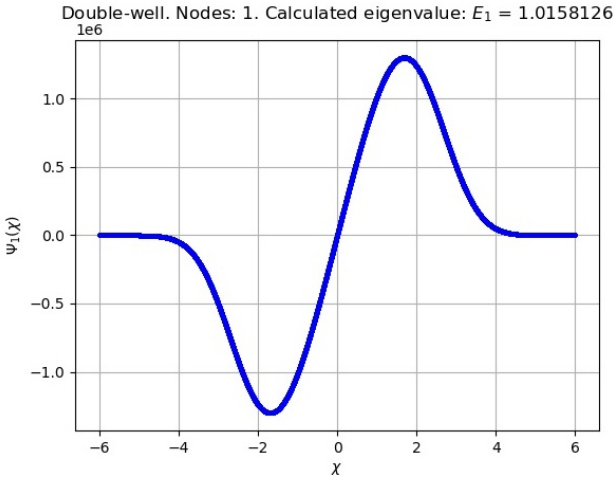

Figure 9: Solution of (20) for $n = 1$.

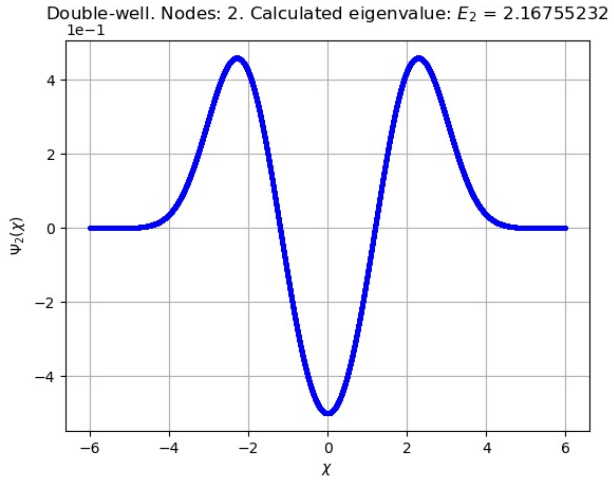

Figure 10: Solution of (20) for $n = 2$.

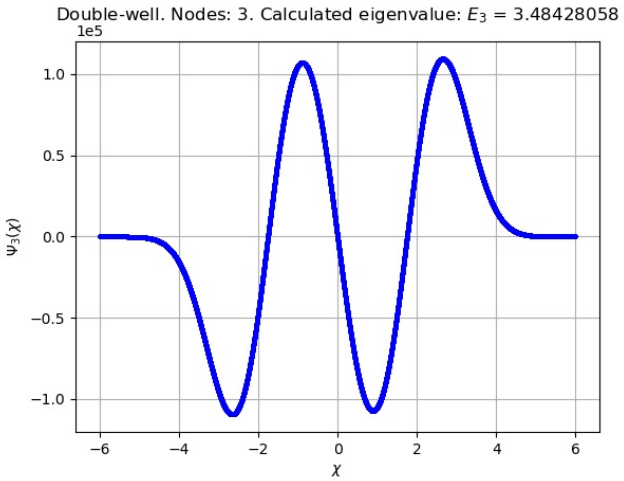

Figure 11: Solution of (20) for $n = 3$.

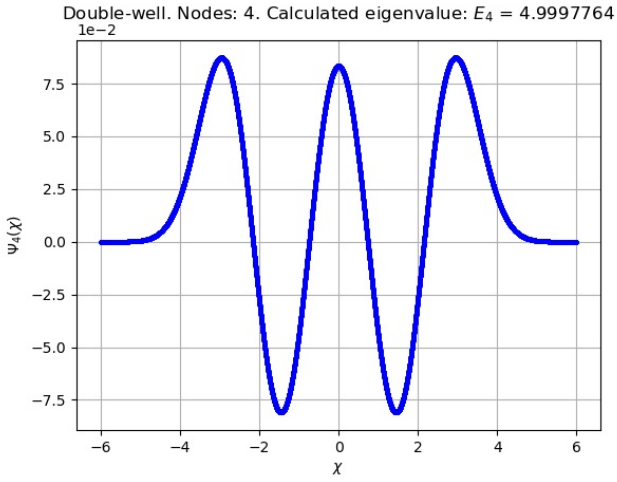

Figure 12: Solution of (20) for $n = 4$.

5 The Morse Potential.

The Morse potential can be used to model the potential energy of a diatomic molecule[4] and can be written as

$$V(r) = D[e^{-2a(r-r_e)} - 2e^{-a(r-r_e)}] \quad , \quad r > 0 \tag{21}$$

where D and a are, not independent, parameters. Then, bound states of the Morse oscillator are solutions $\Psi_n(r)$ and E_n to the following Schrödinger equation:

$$-\frac{\hbar}{2m}\frac{d^2}{dr^2}\Psi_n(r) = [E_n - V(r)]\Psi_n(r) \tag{22}$$

where $V(r)$ is given by (21). A change of variables will be introduced to work with dimensionless quantities. Namely, introducing

$$x = ar \quad , \quad x_e = ar_e \quad , \quad \lambda = \frac{\sqrt{2mD}}{a\hbar} \quad , \quad \xi_n = \frac{2m}{a^2\hbar^2}E_n \tag{23}$$

(22) and (21) become, respectively:

$$\frac{d^2}{dx^2}\Psi_n(x) = -[\xi_n - V(x)]\Psi_n(x) \tag{24}$$

and

$$V(x) = \lambda^2[e^{-2(x-x_e)} - 2e^{-(x-x_e)}]. \tag{25}$$

Now, equation (24) with potential given by (25) can be solved exactly[4]. Its solution, eigenvalues and eigenfunctions, can be written[5], respectively, as

$$\xi_n = -\left(\lambda - n - \frac{1}{2}\right)^2 \quad , \quad n = 0, 1, ..., \left\lfloor \lambda - \frac{1}{2} \right\rfloor \tag{26}$$

where $\lfloor x \rfloor$ denotes the floor function, and

$$\Psi_n(z) = N_n z^{\lambda - n - \frac{1}{2}} e^{-\frac{1}{2}z} L_n^{(2\lambda - 2n - 1)}(z) \quad , \quad \text{with} \quad z = 2\lambda e^{-(x - x_e)} \tag{27}$$

where $L_n^{(\alpha)}(z)$ are the generalized, or associated, Laguerre polynomials; N_n and $L_n^{(\alpha)}(z)$ are given by:

$$N_n = \left[\frac{n!(2\lambda - 2n - 1)}{\Gamma(2\lambda - n)} \right]^{\frac{1}{2}} \quad , \quad L_n^{(\alpha)}(z) = \frac{e^z z^{-\alpha}}{n!} \frac{d^n}{dz^n} \left(z^{n+\alpha} e^{-z} \right) \tag{28}$$

where $\Gamma(x)$ is the Gamma function.

Finally, the potential chosen was for $\lambda = 5$ and $x_e = 3$. Then, (25) and (26) take the form

$$V(x) = 25[e^{-2(x-3)} - 2e^{-(x-3)}] \quad , \quad \xi_n = -\left(\frac{9}{2} - n \right)^2 \quad , \quad n = 0, 1, ..., 4 \tag{29}$$

and the wave function is:

$$\Psi_n(z) = N_n z^{\frac{9}{2} - n} e^{-\frac{1}{2}z} L_n^{(9-2n)}(z), \quad \text{with} \quad z = 10e^{-(x-3)} \quad \text{and} \quad N_n = \left[\frac{n!(9 - 2n)}{\Gamma(10 - n)} \right]^{\frac{1}{2}} \tag{30}$$

That value for λ was chosen because it gives a reasonable number of bound states for the value of x_e. The potential for these values can be seen in Figure 13.

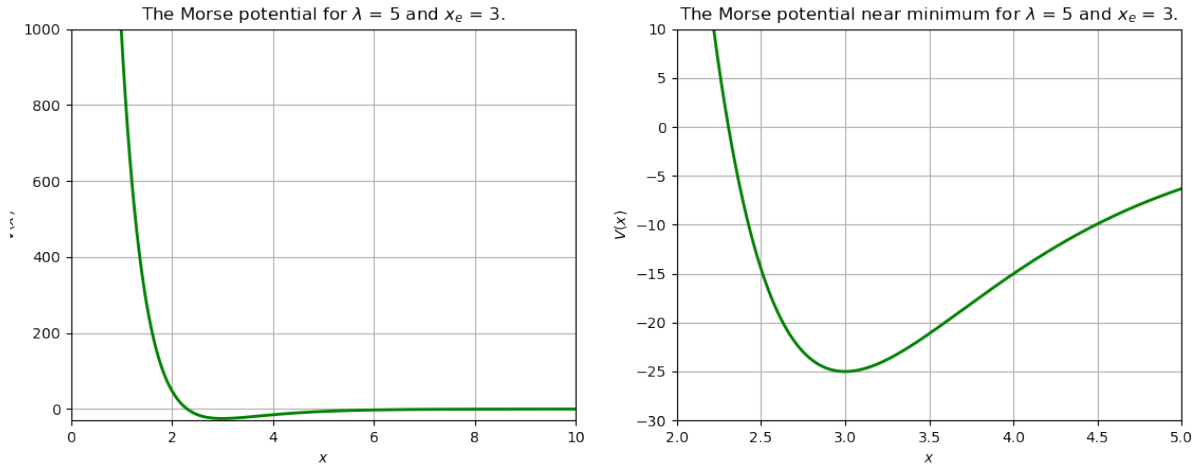

Figure 13: The Morse potential for $\lambda = 5$ and $x_e = 3$.

Given the shape[4] of the solutions to equation (24) we can set[6]:

$$y_0 = 0 \quad , \quad y_1 = \pm \frac{(\Delta x)^2}{12} \tag{31}$$

where we take the negative sign for odd number of nodes, and we take the plus sign for the other cases, namely zero and even number of nodes.

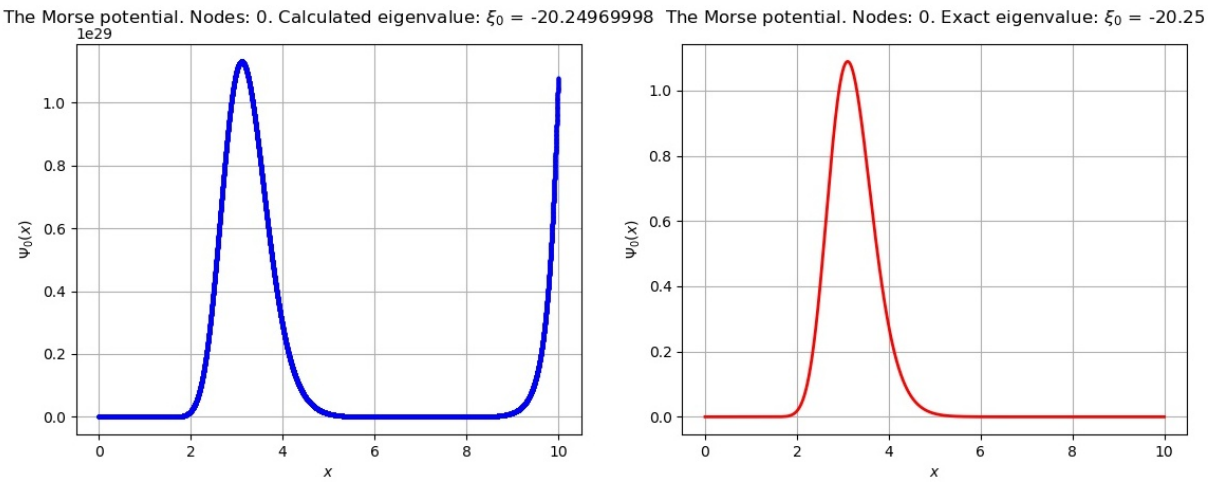

Figure 14: Solution of (24) for (25) with $\lambda = 5$ and $x_e = 3$ for $n = 0$. Left: solution obtained. Right: exact solution.

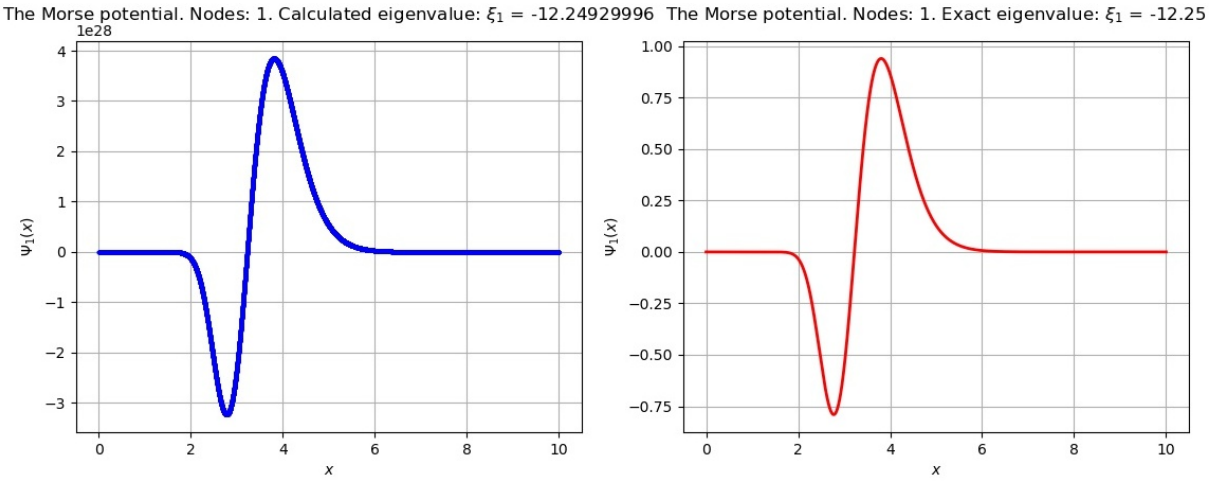

Figure 15: Solution of (24) for (25) with $\lambda = 5$ and $x_e = 3$ for $n = 1$. Left: solution obtained. Right: exact solution.

For every calculation, the value for upper bound of the interval was chosen to be 10. This is because 10 assures the decay towards zero of the potential and graphing the solutions over that interval preserves (mostly) their shape. The exception to this is are three and four nodes. In these cases 10 forced the solutions to go to zero at $x = 10$ and gave an incorrect eigenvalues, and eigenfunctions, so 15 and 20 were chosen, respectively, instead. All five possible solutions were calculated.

Results and comparison with exact solution can be seen in Figures 14, 15, 16, 17 and 18.

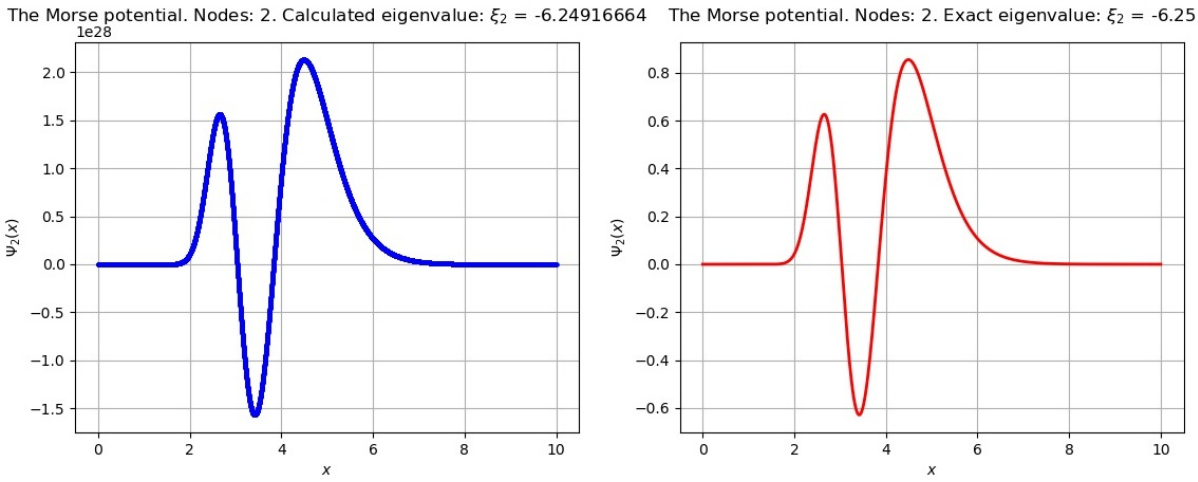

Figure 16: Solution of (24) for (25) with $\lambda = 5$ and $x_e = 3$ for $n = 2$. Left: solution obtained. Right: exact solution.

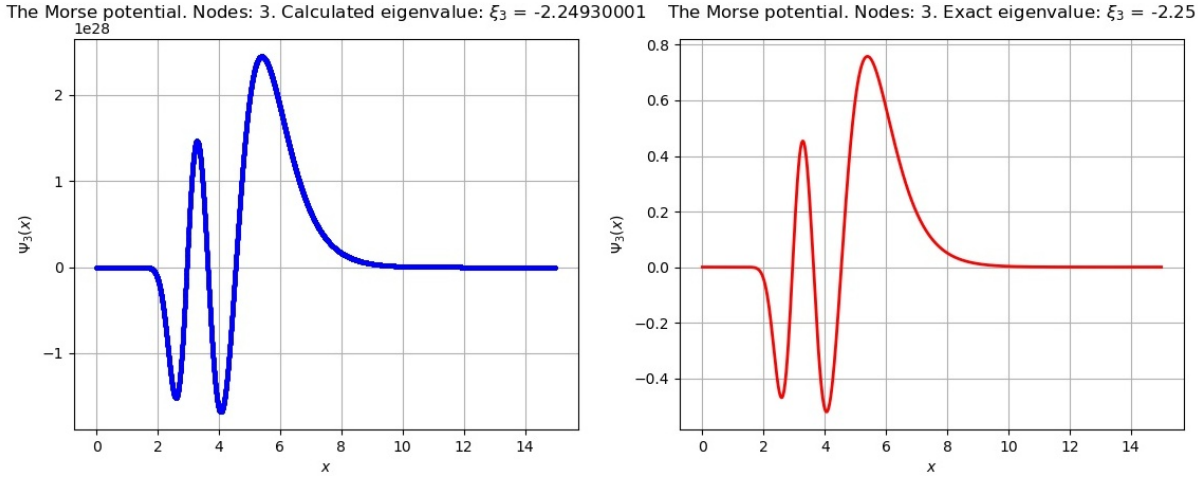

Figure 17: Solution of (24) for (25) with $\lambda = 5$ and $x_e = 3$ for $n = 3$. Left: solution obtained. Right: exact solution.

6 Discussion.

As mentioned previously, solutions obtained will tend to diverge for large values of x. This happens because we only integrate forwards from zero[1]. We could prevent this by doing another integration, backwards, from the upper bound of the interval, and then matching both solutions to get a continuous wave function[6]. This would allow normalizable solutions.

For the harmonic and double-well potentials, this can't be seen because we restricted the interval to one where we could appreciate the solutions. However, for the ground state of the Morse potential, this behaviour can be clearly seen in Figure 14. We can't see this in the excited states because of the scale of the y-axis, we are looking at numbers of order 30 i.e., 10^{30}.

This is the main problem of this method, stability when the wave function goes to zero.

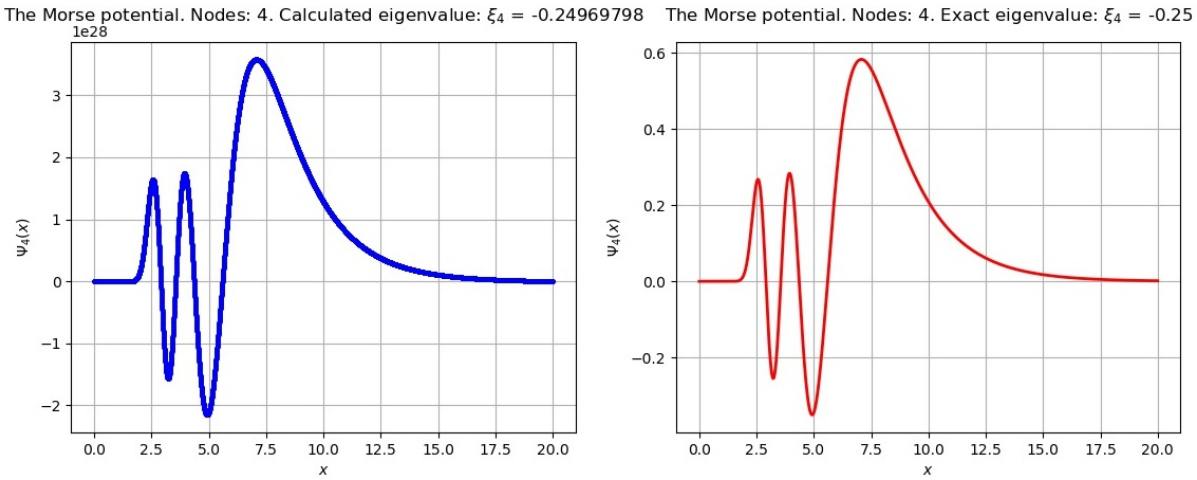

Figure 18: Solution of (24) for (25) with $\lambda = 5$ and $x_e = 3$ for $n = 4$. Left: solution obtained. Right: exact solution.

Otherwise, the algorithm works very well. We can see that, aside from normalization, the shape of the solutions are nearly identical to the exact solutions[3]. This stems from Equation (4), where we can see that we are ignoring terms of order $(\Delta x)^6$. Thus, for a step small enough, the solution gets extremely accurate.

Another issue we might come across is that, for larger number of nodes, the algorithm requires an increasingly larger number of points in the grid. This could be a problem for other potentials, that allow more bounded states or require the interval to be bigger, or both. But for the first couple of bounded states it works great.

Numerov's method achieves what it's set to do as it gives accurate solutions for both the eigenfunctions and the eigenvalues. The biggest issue with it is that the solutions obtained tend to diverge where the function is vanishingly small. This can be fixed by integrating from both ends of the interval and matching both solutions.

References

[1] Giannozzi, P. (2019) "*Numerical Methods in Quantum Mechanics*". Lecture notes. University of Udine, Italy. Academic year 2018/2019.

[2] Merzbacher, E. (1998) "*Quantum Mechanics*". United States of America: John Wiley & Sons, Ltd.

[3] Sitnitsky, A.E. (2018). "*Analytic calculation of ground state splitting in symmetric double well potential*". Computational and Theoretical Chemistry, 1138, 15-22.

[4] Dahl, J. P., & Springborg, M. (1988). "*The Morse oscillator in position space, momentum space, and phase space*". Journal of Chemical Physics, 88(7), 4535-4547. https://doi.org/10.1063/1.453761

[5] Morse potential. (n.d.). In *Wikipedia*. Retrieved September 5, 2019, from https://en.wikipedia.org/wiki/Morse_potential

[6] Kenhere, D. G. (n.d.) "*Bound State of One Dimensional Potential by Numerov Method* ". Department of Physics and Centre for Modeling and Simulation of the University of Pune, India.